

Search for Charged Higgs Bosons from Top Quark Decays in $p\bar{p}$ Collisions at $\sqrt{s} = 1.96$ TeV

A. Abulencia,²³ D. Acosta,¹⁷ J. Adelman,¹³ T. Affolder,¹⁰ T. Akimoto,⁵³ M. G. Albrow,¹⁶ D. Ambrose,¹⁶ S. Amerio,⁴² D. Amidei,³³ A. Anastassov,⁵⁰ K. Anikeev,¹⁶ A. Annovi,⁴⁴ J. Antos,¹ M. Aoki,⁵³ G. Apollinari,¹⁶ J.-F. Arguin,³² T. Arisawa,⁵⁵ A. Artikov,¹⁴ W. Ashmanskas,¹⁶ A. Attal,⁸ F. Azfar,⁴¹ P. Azzi-Bacchetta,⁴² P. Azzurri,⁴⁴ N. Bacchetta,⁴² H. Bachacou,²⁸ W. Badgett,¹⁶ A. Barbaro-Galtieri,²⁸ V. E. Barnes,⁴⁶ B. A. Barnett,²⁴ S. Baroiant,⁷ V. Bartsch,³⁰ G. Bauer,³¹ F. Bedeschi,⁴⁴ S. Behari,²⁴ S. Belforte,⁵² G. Bellettini,⁴⁴ J. Bellinger,⁵⁷ A. Belloni,³¹ E. Ben-Haim,¹⁶ D. Benjamin,¹⁵ A. Beretvas,¹⁶ J. Beringer,²⁸ T. Berry,²⁹ A. Bhatti,⁴⁸ M. Binkley,¹⁶ D. Bisello,⁴² M. Bishai,¹⁶ R. E. Blair,² C. Blocker,⁶ K. Bloom,³³ B. Blumenfeld,²⁴ A. Bocci,⁴⁸ A. Bodek,⁴⁷ V. Boisvert,⁴⁷ G. Bolla,⁴⁶ A. Bolshov,³¹ D. Bortoletto,⁴⁶ J. Boudreau,⁴⁵ S. Bourov,¹⁶ A. Boveia,¹⁰ B. Brau,¹⁰ C. Bromberg,³⁴ E. Brubaker,¹³ J. Budagov,¹⁴ H. S. Budd,⁴⁷ S. Budd,²³ K. Burkett,¹⁶ G. Busetto,⁴² P. Bussey,²⁰ K. L. Byrum,² S. Cabrera,¹⁵ M. Campanelli,¹⁹ M. Campbell,³³ F. Canelli,⁸ A. Canepa,⁴⁶ D. Carlsmith,⁵⁷ R. Carosi,⁴⁴ S. Carron,¹⁵ M. Casarsa,⁵² A. Castro,⁵ P. Catastini,⁴⁴ D. Cauz,⁵² M. Cavalli-Sforza,³ A. Cerri,²⁸ L. Cerrito,⁴¹ S. H. Chang,²⁷ J. Chapman,³³ Y. C. Chen,¹ M. Chertok,⁷ G. Chiarelli,⁴⁴ G. Chlachidze,¹⁴ F. Chlebana,¹⁶ I. Cho,²⁷ K. Cho,²⁷ D. Chokheli,¹⁴ J. P. Chou,²¹ P. H. Chu,²³ S. H. Chuang,⁵⁷ K. Chung,¹² W. H. Chung,⁵⁷ Y. S. Chung,⁴⁷ M. Ciljak,⁴⁴ C. I. Ciobanu,²³ M. A. Ciocci,⁴⁴ A. Clark,¹⁹ D. Clark,⁶ M. Coca,¹⁵ A. Connolly,²⁸ M. E. Convery,⁴⁸ J. Conway,⁷ B. Cooper,³⁰ K. Copic,³³ M. Cordelli,¹⁸ G. Cortiana,⁴² A. Cruz,¹⁷ J. Cuevas,¹¹ R. Culbertson,¹⁶ D. Cyr,⁵⁷ S. DaRonco,⁴² S. D'Auria,²⁰ M. D'onofrio,¹⁹ D. Dagenhart,⁶ P. de Barbaro,⁴⁷ S. De Cecco,⁴⁹ A. Deisher,²⁸ G. De Lentdecker,⁴⁷ M. Dell'Orso,⁴⁴ S. Demers,⁴⁷ L. Demortier,⁴⁸ J. Deng,¹⁵ M. Deninno,⁵ D. De Pedis,⁴⁹ P. F. Derwent,¹⁶ C. Dionisi,⁴⁹ J. R. Dittmann,⁴ P. DiTuro,⁵⁰ C. Dörr,²⁵ A. Dominguez,²⁸ S. Donati,⁴⁴ M. Donega,¹⁹ P. Dong,⁸ J. Donini,⁴² T. Dorigo,⁴² S. Dube,⁵⁰ K. Ebina,⁵⁵ J. Efron,³⁸ J. Ehlers,¹⁹ R. Erbacher,⁷ D. Errede,²³ S. Errede,²³ R. Eusebi,⁴⁷ H. C. Fang,²⁸ S. Farrington,²⁹ I. Fedorko,⁴⁴ W. T. Fedorko,¹³ R. G. Feild,⁵⁸ M. Feindt,²⁵ J. P. Fernandez,⁴⁶ R. Field,¹⁷ G. Flanagan,³⁴ L. R. Flores-Castillo,⁴⁵ A. Foland,²¹ S. Forrester,⁷ G. W. Foster,¹⁶ M. Franklin,²¹ J. C. Freeman,²⁸ Y. Fujii,²⁶ I. Furic,¹³ A. Gajjar,²⁹ M. Gallinaro,⁴⁸ J. Galyardt,¹² J. E. Garcia,⁴⁴ M. Garcia Sciveres,²⁸ A. F. Garfinkel,⁴⁶ C. Gay,⁵⁸ H. Gerberich,²³ E. Gerchtein,¹² D. Gerdes,³³ S. Giagu,⁴⁹ P. Giannetti,⁴⁴ A. Gibson,²⁸ K. Gibson,¹² C. Ginsburg,¹⁶ K. Giolo,⁴⁶ M. Giordani,⁵² M. Giunta,⁴⁴ G. Giurgiu,¹² V. Glagolev,¹⁴ D. Glenzinski,¹⁶ M. Gold,³⁶ N. Goldschmidt,³³ J. Goldstein,⁴¹ G. Gomez,¹¹ G. Gomez-Ceballos,¹¹ M. Goncharov,⁵¹ O. González,⁴⁶ I. Gorelov,³⁶ A. T. Goshaw,¹⁵ Y. Gotra,⁴⁵ K. Goulianos,⁴⁸ A. Gresele,⁴² M. Griffiths,²⁹ S. Grinstein,²¹ C. Grosso-Pilcher,¹³ U. Grundler,²³ J. Guimaraes da Costa,²¹ C. Haber,²⁸ S. R. Hahn,¹⁶ K. Hahn,⁴³ E. Halkiadakis,⁴⁷ A. Hamilton,³² B.-Y. Han,⁴⁷ R. Handler,⁵⁷ F. Happacher,¹⁸ K. Hara,⁵³ M. Hare,⁵⁴ S. Harper,⁴¹ R. F. Harr,⁵⁶ R. M. Harris,¹⁶ K. Hatakeyama,⁴⁸ J. Hauser,⁸ C. Hays,¹⁵ H. Hayward,²⁹ A. Heijboer,⁴³ B. Heinemann,²⁹ J. Heinrich,⁴³ M. Hennecke,²⁵ M. Herndon,⁵⁷ J. Heuser,²⁵ D. Hidas,¹⁵ C. S. Hill,¹⁰ D. Hirschbuehl,²⁵ A. Hocker,¹⁶ A. Holloway,²¹ S. Hou,¹ M. Houlden,²⁹ S.-C. Hsu,⁹ B. T. Huffman,⁴¹ R. E. Hughes,³⁸ J. Huston,³⁴ K. Ikado,⁵⁵ J. Incandela,¹⁰ G. Introzzi,⁴⁴ M. Iori,⁴⁹ Y. Ishizawa,⁵³ A. Ivanov,⁷ B. Iyutin,³¹ E. James,¹⁶ D. Jang,⁵⁰ B. Jayatilaka,³³ D. Jeans,⁴⁹ H. Jensen,¹⁶ E. J. Jeon,²⁷ M. Jones,⁴⁶ K. K. Joo,²⁷ S. Y. Jun,¹² T. R. Junk,²³ T. Kamon,⁵¹ J. Kang,³³ M. Karagoz-Unel,³⁷ P. E. Karchin,⁵⁶ Y. Kato,⁴⁰ Y. Kemp,²⁵ R. Kephart,¹⁶ U. Kerzel,²⁵ V. Khotilovich,⁵¹ B. Kilminster,³⁸ D. H. Kim,²⁷ H. S. Kim,²⁷ J. E. Kim,²⁷ M. J. Kim,¹² M. S. Kim,²⁷ S. B. Kim,²⁷ S. H. Kim,⁵³ Y. K. Kim,¹³ M. Kirby,¹⁵ L. Kirsch,⁶ S. Klimentenko,¹⁷ M. Klute,³¹ B. Knuteson,³¹ B. R. Ko,¹⁵ H. Kobayashi,⁵³ K. Kondo,⁵⁵ D. J. Kong,²⁷ J. Konigsberg,¹⁷ K. Kordas,¹⁸ A. Korytov,¹⁷ A. V. Kotwal,¹⁵ A. Kovalev,⁴³ J. Kraus,²³ I. Kravchenko,³¹ M. Kreps,²⁵ A. Kreymer,¹⁶ J. Kroll,⁴³ N. Krumnack,⁴ M. Kruse,¹⁵ V. Krutelyov,⁵¹ S. E. Kuhlmann,² Y. Kusakabe,⁵⁵ S. Kwang,¹³ A. T. Laasanen,⁴⁶ S. Lai,³² S. Lami,⁴⁴ S. Lammel,¹⁶ M. Lancaster,³⁰ R. L. Lander,⁷ K. Lannon,³⁸ A. Lath,⁵⁰ G. Latino,⁴⁴ I. Lazzizzera,⁴² C. Lecci,²⁵ T. LeCompte,² J. Lee,⁴⁷ J. Lee,²⁷ S. W. Lee,⁵¹ R. Lefèvre,³ N. Leonardo,³¹ S. Leone,⁴⁴ S. Levy,¹³ J. D. Lewis,¹⁶ K. Li,⁵⁸ C. Lin,⁵⁸ C. S. Lin,¹⁶ M. Lindgren,¹⁶ E. Lipeles,⁹ T. M. Liss,²³ A. Lister,¹⁹ D. O. Litvintsev,¹⁶ T. Liu,¹⁶ Y. Liu,¹⁹ N. S. Lockyer,⁴³ A. Loginov,³⁵ M. Loreti,⁴² P. Loverre,⁴⁹ R.-S. Lu,¹ D. Lucchesi,⁴² P. Lujan,²⁸ P. Lukens,¹⁶ G. Lungu,¹⁷ L. Lyons,⁴¹ J. Lys,²⁸ R. Lysak,¹ E. Lytken,⁴⁶ P. Mack,²⁵ D. MacQueen,³² R. Madrak,¹⁶ K. Maeshima,¹⁶ P. Maksimovic,²⁴ G. Manca,²⁹ F. Margaroli,⁵ R. Marginean,¹⁶ C. Marino,²³ A. Martin,⁵⁸ M. Martin,²⁴ V. Martin,³⁷ M. Martínez,³ T. Maruyama,⁵³ H. Matsunaga,⁵³ M. E. Mattson,⁵⁶ R. Mazini,³² P. Mazzanti,⁵ K. S. McFarland,⁴⁷ D. McGivern,³⁰ P. McIntyre,⁵¹ P. McNamara,⁵⁰ R. McNulty,²⁹ A. Mehta,²⁹ S. Menzemer,³¹ A. Menzione,⁴⁴ P. Merkel,⁴⁶ C. Mesropian,⁴⁸ A. Messina,⁴⁹ M. von der Mey,⁸ T. Miao,¹⁶ N. Miladinovic,⁶ J. Miles,³¹ R. Miller,³⁴ J. S. Miller,³³ C. Mills,¹⁰ M. Milnik,²⁵ R. Miquel,²⁸ S. Miscetti,¹⁸ G. Mitselmakher,¹⁷ A. Miyamoto,²⁶ N. Moggi,⁵ B. Mohr,⁸ R. Moore,¹⁶ M. Morello,⁴⁴ P. Movilla Fernandez,²⁸ J. Mülmenstädt,²⁸ A. Mukherjee,¹⁶ M. Mulhearn,³¹ Th. Muller,²⁵ R. Mumford,²⁴ P. Murat,¹⁶ J. Nachtman,¹⁶ S. Nahn,⁵⁸ I. Nakano,³⁹

A. Napier,⁵⁴ D. Naumov,³⁶ V. Necula,¹⁷ C. Neu,⁴³ M. S. Neubauer,⁹ J. Nielsen,²⁸ T. Nigmanov,⁴⁵ L. Nodulman,² O. Norriella,³ T. Ogawa,⁵⁵ S. H. Oh,¹⁵ Y. D. Oh,²⁷ T. Okusawa,⁴⁰ R. Oldeman,²⁹ R. Orava,²² K. Osterberg,²² C. Pagliarone,⁴⁴ E. Palencia,¹¹ R. Paoletti,⁴⁴ V. Papadimitriou,¹⁶ A. Papikononou,²⁵ A. A. Paramonov,¹³ B. Parks,³⁸ S. Pashapour,³² J. Patrick,¹⁶ G. Pauletta,⁵² M. Paulini,¹² C. Paus,³¹ D. E. Pellett,⁷ A. Penzo,⁵² T. J. Phillips,¹⁵ G. Piacentino,⁴⁴ J. Piedra,¹¹ K. Pitts,²³ C. Plager,⁸ L. Pondrom,⁵⁷ G. Pope,⁴⁵ X. Portell,³ O. Poukhov,¹⁴ N. Pounder,⁴¹ F. Prakooshyn,¹⁴ A. Pronko,¹⁶ J. Proudfoot,² F. Ptohos,¹⁸ G. Punzi,⁴⁴ J. Pursley,²⁴ J. Rademacker,⁴¹ A. Rahaman,⁴⁵ A. Rakitin,³¹ S. Rappoccio,²¹ F. Ratnikov,⁵⁰ B. Reiser,¹⁶ V. Rekovic,³⁶ N. van Remortel,²² P. Renton,⁴¹ M. Rescigno,⁴⁹ S. Richter,²⁵ F. Rimondi,⁵ K. Rinnert,²⁵ L. Ristori,⁴⁴ W. J. Robertson,¹⁵ A. Robson,²⁰ T. Rodrigo,¹¹ E. Rogers,²³ S. Rolli,⁵⁴ R. Roser,¹⁶ M. Rossi,⁵² R. Rossin,¹⁷ C. Rott,⁴⁶ A. Ruiz,¹¹ J. Russ,¹² V. Rusu,¹³ D. Ryan,⁵⁴ H. Saarikko,²² S. Sabik,³² A. Safonov,⁷ W. K. Sakumoto,⁴⁷ G. Salamanna,⁴⁹ O. Salto,³ D. Saltzberg,⁸ C. Sanchez,³ L. Santi,⁵² S. Sarkar,⁴⁹ K. Sato,⁵³ P. Savard,³² A. Savoy-Navarro,¹⁶ T. Scheidle,²⁵ P. Schlabach,¹⁶ E. E. Schmidt,¹⁶ M. P. Schmidt,⁵⁸ M. Schmitt,³⁷ T. Schwarz,³³ L. Scodellaro,¹¹ A. L. Scott,¹⁰ A. Scribano,⁴⁴ F. Scuri,⁴⁴ A. Sedov,⁴⁶ S. Seidel,³⁶ Y. Seiya,⁴⁰ A. Semenov,¹⁴ F. Semeria,⁵ L. Sexton-Kennedy,¹⁶ I. Sfiligoi,¹⁸ M. D. Shapiro,²⁸ T. Shears,²⁹ P. F. Shepard,⁴⁵ D. Sherman,²¹ M. Shimojima,⁵³ M. Shochet,¹³ Y. Shon,⁵⁷ I. Shreyber,³⁵ A. Sidoti,⁴⁴ A. Sill,¹⁶ P. Sinervo,³² A. Sisakyan,¹⁴ J. Sjolin,⁴¹ A. Skiba,²⁵ A. J. Slaughter,¹⁶ K. Sliwa,⁵⁴ D. Smirnov,³⁶ J. R. Smith,⁷ F. D. Snider,¹⁶ R. Snihur,³² M. Soderberg,³³ A. Soha,⁷ S. Somalwar,⁵⁰ V. Sorin,³⁴ J. Spalding,¹⁶ F. Spinella,⁴⁴ P. Squillacioti,⁴⁴ M. Stanitzki,⁵⁸ A. Staveris-Polykalas,⁴⁴ R. St. Denis,²⁰ B. Stelzer,⁸ O. Stelzer-Chilton,³² D. Stentz,³⁷ J. Strogos,³⁶ D. Stuart,¹⁰ J. S. Suh,²⁷ A. Sukhanov,¹⁷ K. Sumorok,³¹ H. Sun,⁵⁴ T. Suzuki,⁵³ A. Taffard,²³ R. Tafirout,³² R. Takashima,³⁹ Y. Takeuchi,⁵³ K. Takikawa,⁵³ M. Tanaka,² R. Tanaka,³⁹ M. Tecchio,³³ P. K. Teng,¹ K. Terashi,⁴⁸ S. Tether,³¹ J. Thom,¹⁶ A. S. Thompson,²⁰ E. Thomson,⁴³ P. Tipton,⁴⁷ V. Tiwari,¹² S. Tkaczyk,¹⁶ D. Toback,⁵¹ K. Tollefson,³⁴ T. Tomura,⁵³ D. Tonelli,⁴⁴ M. Tönnemann,³⁴ S. Torre,⁴⁴ D. Torretta,¹⁶ S. Tourneur,¹⁶ W. Trischuk,³² R. Tsuchiya,⁵⁵ S. Tsuno,³⁹ N. Turini,⁴⁴ F. Ukegawa,⁵³ T. Unverhau,²⁰ S. Uozumi,⁵³ D. Usynin,⁴³ L. Vacavant,²⁸ A. Vaiciulis,⁴⁷ S. Vallecorsa,¹⁹ A. Varganov,³³ E. Vataga,³⁶ G. Velez,¹⁶ G. Veramendi,²³ V. Veszpremi,⁴⁶ T. Vickey,²³ R. Vidal,¹⁶ I. Vila,¹¹ R. Vilar,¹¹ I. Vollrath,³² I. Volobouev,²⁸ F. Würthwein,⁹ P. Wagner,⁵¹ R. G. Wagner,² R. L. Wagner,¹⁶ W. Wagner,²⁵ R. Wallny,⁸ T. Walter,²⁵ Z. Wan,⁵⁰ M. J. Wang,¹ S. M. Wang,¹⁷ A. Warburton,³² B. Ward,²⁰ S. Waschke,²⁰ D. Waters,³⁰ T. Watts,⁵⁰ M. Weber,²⁸ W. C. Wester III,¹⁶ B. Whitehouse,⁵⁴ D. Whiteson,⁴³ A. B. Wicklund,² E. Wicklund,¹⁶ H. H. Williams,⁴³ P. Wilson,¹⁶ B. L. Winer,³⁸ P. Wittich,⁴³ S. Wolbers,¹⁶ C. Wolfe,¹³ S. Worm,⁵⁰ T. Wright,³³ X. Wu,¹⁹ S. M. Wynne,²⁹ A. Yagil,¹⁶ K. Yamamoto,⁴⁰ J. Yamaoka,⁵⁰ Y. Yamashita,³⁹ C. Yang,⁵⁸ U. K. Yang,¹³ W. M. Yao,²⁸ G. P. Yeh,¹⁶ J. Yoh,¹⁶ K. Yorita,¹³ T. Yoshida,⁴⁰ I. Yu,²⁷ S. S. Yu,⁴³ J. C. Yun,¹⁶ L. Zanello,⁴⁹ A. Zanetti,⁵² I. Zaw,²¹ F. Zetti,⁴⁴ X. Zhang,²³ J. Zhou,⁵⁰ and S. Zucchelli⁵

(CDF Collaboration)

¹*Institute of Physics, Academia Sinica, Taipei, 11529 Taiwan, Republic of China*²*Argonne National Laboratory, Argonne, Illinois 60439, USA*³*Institut de Fisica d'Altes Energies, Universitat Autònoma de Barcelona, E-08193, Bellaterra (Barcelona), Spain*⁴*Baylor University, Waco, Texas 76798, USA*⁵*Istituto Nazionale di Fisica Nucleare, University of Bologna, I-40127 Bologna, Italy*⁶*Brandeis University, Waltham, Massachusetts 02254, USA*⁷*University of California–Davis, Davis, California 95616, USA*⁸*University of California–Los Angeles, Los Angeles, California 90024, USA*⁹*University of California–San Diego, La Jolla, California 92093, USA*¹⁰*University of California–Santa Barbara, Santa Barbara, California 93106, USA*¹¹*Instituto de Fisica de Cantabria, CSIC-University of Cantabria, 39005 Santander, Spain*¹²*Carnegie Mellon University, Pittsburgh, Pennsylvania 15213, USA*¹³*Enrico Fermi Institute, University of Chicago, Chicago, Illinois 60637, USA*¹⁴*Joint Institute for Nuclear Research, RU-141980 Dubna, Russia*¹⁵*Duke University, Durham, North Carolina 27708, USA*¹⁶*Fermi National Accelerator Laboratory, Batavia, Illinois 60510, USA*¹⁷*University of Florida, Gainesville, Florida 32611, USA*¹⁸*Laboratori Nazionali di Frascati, Istituto Nazionale di Fisica Nucleare, I-00044 Frascati, Italy*¹⁹*University of Geneva, CH-1211 Geneva 4, Switzerland*²⁰*Glasgow University, Glasgow G12 8QQ, United Kingdom*²¹*Harvard University, Cambridge, Massachusetts 02138, USA*

- ²²*Division of High Energy Physics, Department of Physics, University of Helsinki and Helsinki Institute of Physics, FIN-00014, Helsinki, Finland*
- ²³*University of Illinois, Urbana, Illinois 61801, USA*
- ²⁴*The Johns Hopkins University, Baltimore, Maryland 21218, USA*
- ²⁵*Institut für Experimentelle Kernphysik, Universität Karlsruhe, 76128 Karlsruhe, Germany*
- ²⁶*High Energy Accelerator Research Organization (KEK), Tsukuba, Ibaraki 305, Japan*
- ²⁷*Center for High Energy Physics: Kyungpook National University, Taegu 702-701; Seoul National University, Seoul 151-742; and SungKyunKwan University, Suwon 440-746; Korea*
- ²⁸*Ernest Orlando Lawrence Berkeley National Laboratory, Berkeley, California 94720, USA*
- ²⁹*University of Liverpool, Liverpool L69 7ZE, United Kingdom*
- ³⁰*University College London, London WC1E 6BT, United Kingdom*
- ³¹*Massachusetts Institute of Technology, Cambridge, Massachusetts 02139, USA*
- ³²*Institute of Particle Physics: McGill University, Montréal, Canada H3A 2T8; and University of Toronto, Toronto, Canada M5S 1A7*
- ³³*University of Michigan, Ann Arbor, Michigan 48109, USA*
- ³⁴*Michigan State University, East Lansing, Michigan 48824, USA*
- ³⁵*Institution for Theoretical and Experimental Physics, ITEP, Moscow 117259, Russia*
- ³⁶*University of New Mexico, Albuquerque, New Mexico 87131, USA*
- ³⁷*Northwestern University, Evanston, Illinois 60208, USA*
- ³⁸*The Ohio State University, Columbus, Ohio 43210, USA*
- ³⁹*Okayama University, Okayama 700-8530, Japan*
- ⁴⁰*Osaka City University, Osaka 588, Japan*
- ⁴¹*University of Oxford, Oxford OX1 3RH, United Kingdom*
- ⁴²*Istituto Nazionale di Fisica Nucleare, Sezione di Padova-Trento, University of Padova, I-35131 Padova, Italy*
- ⁴³*University of Pennsylvania, Philadelphia, Pennsylvania 19104, USA*
- ⁴⁴*Istituto Nazionale di Fisica Nucleare Pisa, Universities of Pisa, Siena and Scuola Normale Superiore, I-56127 Pisa, Italy*
- ⁴⁵*University of Pittsburgh, Pittsburgh, Pennsylvania 15260, USA*
- ⁴⁶*Purdue University, West Lafayette, Indiana 47907, USA*
- ⁴⁷*University of Rochester, Rochester, New York 14627, USA*
- ⁴⁸*The Rockefeller University, New York, New York 10021, USA*
- ⁴⁹*Istituto Nazionale di Fisica Nucleare, Sezione di Roma 1, University of Rome "La Sapienza," I-00185 Roma, Italy*
- ⁵⁰*Rutgers University, Piscataway, New Jersey 08855, USA*
- ⁵¹*Texas A&M University, College Station, Texas 77843, USA*
- ⁵²*Istituto Nazionale di Fisica Nucleare, University of Trieste/Udine, Italy*
- ⁵³*University of Tsukuba, Tsukuba, Ibaraki 305, Japan*
- ⁵⁴*Tufts University, Medford, Massachusetts 02155, USA*
- ⁵⁵*Waseda University, Tokyo 169, Japan*
- ⁵⁶*Wayne State University, Detroit, Michigan 48201, USA*
- ⁵⁷*University of Wisconsin, Madison, Wisconsin 53706, USA*
- ⁵⁸*Yale University, New Haven, Connecticut 06520, USA*
- (Received 24 October 2005; published 3 February 2006)

We report the results of a search for a charged Higgs boson in the decays of top quarks produced in $p\bar{p}$ collisions at a center-of-mass energy of 1.96 TeV. We use a data sample corresponding to an integrated luminosity of 193 pb^{-1} collected by the upgraded Collider Detector at Fermilab. No evidence for charged Higgs production is found, allowing 95% C.L. upper limits to be placed on $\text{BR}(t \rightarrow H^\pm b)$ for different charged Higgs decay scenarios. In addition, we present in the minimal supersymmetric standard model ($m_{H^\pm}, \tan\beta$) plane the first exclusion regions with radiative and Yukawa coupling corrections.

DOI: [10.1103/PhysRevLett.96.042003](https://doi.org/10.1103/PhysRevLett.96.042003)

PACS numbers: 14.65.Ha, 14.80.Cp, 13.85.Qk

One of the open questions in the standard model (SM) of particle physics involves the mechanism of electroweak symmetry breaking (EWSB). Within the SM, it is postulated that a single scalar doublet field breaks the symmetry, resulting in a single observable particle of unknown mass called the Higgs boson [1]. To date, the SM Higgs boson has not been observed, and extensions of the SM have been proposed with different Higgs phenomenologies. The sim-

plest extension of the SM Higgs sector introduces another Higgs doublet. In two-Higgs doublet models, EWSB results in five Higgs bosons, three of which are neutral (h^0, H^0, A^0) and two of which are charged (H^\pm). The minimal supersymmetric extension of the SM (MSSM) includes a two-Higgs doublet sector, in which one doublet couples to the up-type quarks and neutrinos and the other to the down-type quarks and charged leptons. The obser-

vation of a charged Higgs boson would provide unambiguous evidence of a Higgs sector richer than that predicted by the SM.

At the Tevatron, direct production of a single charged Higgs is expected to be negligible, and the direct production of H^+H^- via the weak interaction is expected to have a relatively small cross section on the order of 0.1 pb [2]. The production of $t\bar{t}$ pairs, with a theoretical production cross section of $6.7^{+0.7}_{-0.9}$ pb [3] for $m_t = 175 \text{ GeV}/c^2$, may offer another source of charged Higgs production. If kinematically allowed, the top quark can decay to H^+b , competing with the SM decay $t \rightarrow W^+b$. This mechanism can provide a larger production rate of charged Higgs and offers a much cleaner signature than that of direct production.

Previous searches for the charged Higgs boson have been performed at $\sqrt{s} = 1.8 \text{ TeV}$ in the $\tau_h + \cancel{E}_T + \text{jets} + \ell$ channels, where the missing energy \cancel{E}_T is defined in Ref. [4], τ_h denotes a tau lepton which decays to hadrons, and where $\ell = e$ or μ in Ref. [5] and $\ell = e, \mu$ or τ_h in Ref. [6]. In the framework of the tauonic Higgs model, in which the charged Higgs decays exclusively to $\bar{\tau}\nu$, these searches set limits directly on $\text{BR}(t \rightarrow H^+b)$ based on the measured production rate. These results are then translated into limits on $\tan\beta$, the ratio of vacuum expectation values of the two-Higgs doublets. Other searches obtained limits in the $(m_{H^\pm}, \tan\beta)$ plane, assuming that the charged Higgs decays only to $\bar{\tau}\nu$ in the $\cancel{E}_T + \text{jets} + \tau_h$ channel in Ref. [7] and assuming that the charged Higgs decays to $\bar{\tau}\nu, c\bar{s}$, and $t^*\bar{b} (\rightarrow W^+b\bar{b})$ in the $\cancel{E}_T + \text{jets} + \ell$ channel with $\ell = e$ or μ in Ref. [8], where t^* is a virtual top quark.

These limits utilize tree-level MSSM predictions of the $t \rightarrow H^+b$ and charged Higgs branching fraction as a function of $\tan\beta$. It is now known that higher-order radiative corrections significantly modify these predictions. The corrections strongly depend on the parameters of the model and are particularly large at high values of $\tan\beta$ [9]. In addition, it is also predicted that, in the low $\tan\beta$ region, the charged Higgs has a sizable branching fraction to W^+h^0 .

CDF has recently reported measurements of the $t\bar{t}$ production cross section in the $\ell + \cancel{E}_T + \text{jets} + X$ channels, where $\ell = e, \mu$ and where $X = \ell$ (the ‘‘dilepton’’ channel), $X = \tau_h$ (‘‘lepton + tau’’), $X = \text{one or more tagged jets}$ [10] (‘‘lepton + jets, ≥ 1 tag’’), and $X = \text{two or more tagged jets}$ (‘‘lepton + jets, ≥ 2 tags’’). These measure-

ments are carried out under the assumption $\text{BR}(t \rightarrow H^+b) = 0$ and use data samples corresponding to an integrated luminosity of up to 193 pb^{-1} [11–13]. In this analysis, we consider the possibility of $t \rightarrow H^+b$ and recast the cross section results to set limits on charged Higgs production. Depending on the top and Higgs branching ratios, the number of expected events in these decay channels can show an excess or deficit with respect to SM expectations.

As published, these measurements allow the categorization of a single event in multiple channels. In this analysis, extra requirements are applied to each channel in order to force the association of every event to a single channel. The $t\bar{t}$ signal acceptance and non- $t\bar{t}$ SM background contribution to each of these exclusive channels are recalculated, and the changes from the original cross section analyses are found to be mostly negligible. The only exception to this is the ≥ 1 tag and ≥ 2 tags lepton + jets channels, where the latter is a proper subset of the former. Removal of this 100% overlap changes the ≥ 1 tag channel to exactly one tag, ‘‘= 1 tag.’’ The results for these new exclusive channels in terms of background, number of observed events, and number of SM-expected events are shown in Table I.

We assume that the charged Higgs boson can decay only to $\bar{\tau}\nu, c\bar{s}, t^*\bar{b}$, or W^+h^0 , leading to five possible decay modes for a single top quark: (i) $t \rightarrow W^+b$, (ii) $t \rightarrow H^+b, H^+ \rightarrow \bar{\tau}\nu$, (iii) $t \rightarrow H^+b, H^+ \rightarrow c\bar{s}$, (iv) $t \rightarrow H^+b, H^+ \rightarrow t^*\bar{b}$, and (v) $t \rightarrow H^+b, H^+ \rightarrow W^+h^0, h^0 \rightarrow b\bar{b}$. Charge conjugated decays are implied. Allowing for a nonzero $\text{BR}(t \rightarrow H^+b)$, the acceptance of the detector for a given $t\bar{t}$ channel k is

$$\mathcal{A}_k = \sum_{i,j=1}^5 B_i B_j \epsilon_{ij,k}(\Gamma_t, \Gamma_{H^\pm}, m_{H^\pm}, m_{h^0}), \quad (1)$$

where $B_i (B_j)$ represent the branching fractions of the top quark (antiquark) to decay via mode i (j) as listed above, and $\epsilon_{ij,k}$ is the efficiency to detect a $t\bar{t}$ event whose top quarks decay via modes i and j in channel k .

The efficiencies $\epsilon_{ij,k}$ are obtained from Monte Carlo (MC) simulation of $t\bar{t}$ events generated with different masses of the top, H^\pm , and h^0 . The MC generator PYTHIA [14] is modified to include the decay $H^+ \rightarrow t^*\bar{b}$ and is used for the generation of the $t\bar{t}$ events. The detector simulation and reconstruction algorithms for muons, electrons, and jets are identical to those used in the SM $t\bar{t}$ cross

TABLE I. Number of events in each exclusive channel from non- $t\bar{t}$ SM background sources, observed in data, and total expected assuming $\sigma_{t\bar{t}}^{\text{prod}} = 6.7 \text{ pb}$ and $\text{BR}(t \rightarrow H^+b) = 0$.

Channel	Background events	Data events	SM-expected events
Dilepton	2.7 ± 0.7	13	10.9 ± 1.4
Lepton + jets, = 1 tag	21.8 ± 3.0	49	54.0 ± 4.3
Lepton + jets, ≥ 2 tags	1.3 ± 0.3	8	10 ± 1
Lepton + tau	1.3 ± 0.2	2	2.3 ± 0.3

section measurements for the four channels. MC efficiencies are scaled for known differences between MC simulation of the detector response and that observed in data. The dependence of the efficiencies on the width of the top quark (Γ_t) and the width of the charged Higgs (Γ_{H^\pm}) is taken into account using the simulated $t\bar{t}$ events. The systematic uncertainties on $\epsilon_{ij,k}$ for the process $t\bar{t} \rightarrow W^+ b W^- \bar{b}$ are listed in Refs. [11–13] and do not differ much for the other possible decay modes.

The expected number of events in channel k is

$$\mu_k = \sigma_{t\bar{t}}^{\text{prod}} \mathcal{A}_k(\rho) \mathcal{L}_k + n_k^{\text{back}}, \quad (2)$$

where $\sigma_{t\bar{t}}^{\text{prod}}$ is the $t\bar{t}$ production cross section and ρ represents a generic model from which the nine quantities (five BR's, Γ_t , Γ_{H^\pm} , m_{H^\pm} , and m_{h^0}) needed to calculate the acceptance \mathcal{A}_k , can be derived. \mathcal{L}_k is the integrated luminosity, and n_k^{back} is the number of expected background events in channel k (shown in Table I). We assume the inclusion of the Higgs sector does not modify the value of the $t\bar{t}$ production cross section and set it to $\sigma_{t\bar{t}}^{\text{prod}} = 6.7 \pm 0.9$ pb.

For each channel, a likelihood is constructed based on the Poisson probability to observe N_k events when a given model predicts μ_k events. Since the four channels were constructed to be mutually exclusive, the product of their likelihoods is taken to form a final likelihood. The correlations of the efficiencies, backgrounds, and systematic uncertainties between channels are taken into account. The posterior probability distribution of the parameter of interest is constructed from the likelihood and a prior probability density.

In the MSSM, the nine quantities needed to calculate the acceptance are predicted from a specific set of MSSM parameters, including m_{H^\pm} and $\tan\beta$. We use the computational package CPSUPERH [15] to compute all the Higgs masses and branching ratios. This program includes QCD, supersymmetric QCD, and supersymmetric electroweak radiative corrections up to the two-loop leading logarithms and applies these corrections to the top and bottom Yukawa couplings. The top branching ratio to charged Higgs is computed with the same level of accuracy from custom code developed in collaboration with the authors of Ref. [9]. In the context of the MSSM with $m_{A^0} < m_{H^\pm}$, CPSUPERH predicts that the H^+ decay to $W^+ A^0$ is non-negligible for masses of H^\pm below $100 \text{ GeV}/c^2$. In this case, CPSUPERH also predicts the mass of the A^0 to be similar to that of the h^0 , and we assume the kinematics of the decay to $W^+ A^0$ to be identical to that of $W^+ h^0$ when the h^0 and A^0 masses are equal. Thus, we assign to the decay $H^+ \rightarrow W^+ h^0$ a branching ratio of $\text{BR}(H^+ \rightarrow W^+ h^0) + \text{BR}(H^+ \rightarrow W^+ A^0)$, effectively considering both decays.

As an example of how a charged Higgs alters the balance between the top decay channels, Fig. 1(a) shows the expected number of events in each of the exclusive channels

as a function of $\tan\beta$ for $m_{H^\pm} = 120 \text{ GeV}/c^2$. The other relevant MSSM parameters are detailed in the caption. The figure demonstrates the excess expected in the lepton + tau channel and the deficit expected in the other channels for large $\tan\beta$ values. For values of $\tan\beta$ around 7, $\text{BR}(t \rightarrow H^+ b)$ goes to zero and the SM expectation for the different channels is recovered. The relationship between the channels changes with charged Higgs mass. Values of $\tan\beta$ which result in a non-self-consistent Higgs sector are reported by CPSUPERH and are shown as the theoretically inaccessible regions in Fig. 1.

Figure 1(b) shows the posterior probability obtained for the four channels when the number of observed events is equal to that expected from the SM. The posterior is obtained by means of a flat prior in $\log_{10}(\tan\beta)$. This prior allows for a smooth variation of the top and charged Higgs branching ratios as a function of $\log_{10}(\tan\beta)$. The probability is integrated over its maximum density region to obtain expected upper and lower limits on $\tan\beta$ at the 95% confidence level (C.L.).

Using the number of events observed in the data and repeating this procedure for different Higgs masses results

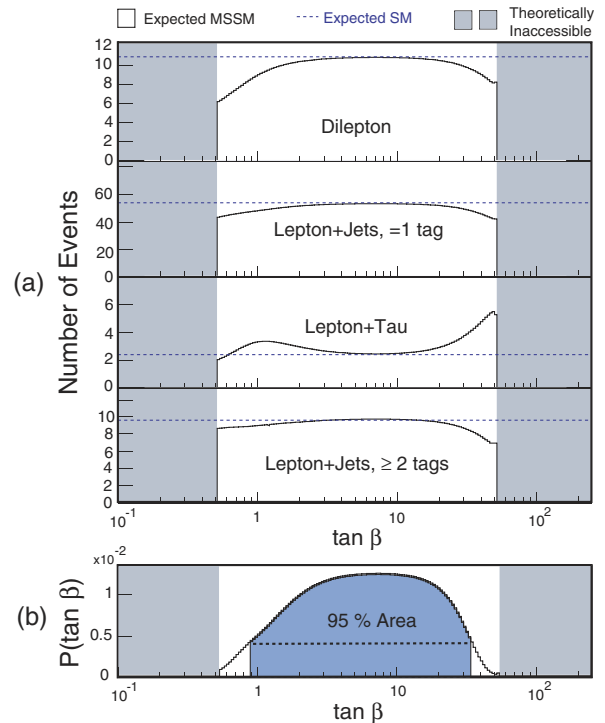


FIG. 1 (color online). Predictions for $m_{H^\pm} = 120 \text{ GeV}/c^2$ and $m_t = 175 \text{ GeV}/c^2$ as a function of $\tan\beta$ for 193 pb^{-1} . The MSSM parameters are defined in Ref. [18] and are set to $M_{\text{SUSY}} = 1000 \text{ GeV}/c^2$, $\mu = -500 \text{ GeV}/c^2$, $A_t = A_b = 2000 \text{ GeV}/c^2$, $A_\tau = 500 \text{ GeV}/c^2$, $M_2 = M_3 = M_Q = M_U = M_D = M_E = M_L = M_{\text{SUSY}}$, and $M_1 = 0.498M_2$. (a) Expected number of events in each of the channels. (b) Posterior probability density obtained when the number of observed events is equal to that expected from the SM.

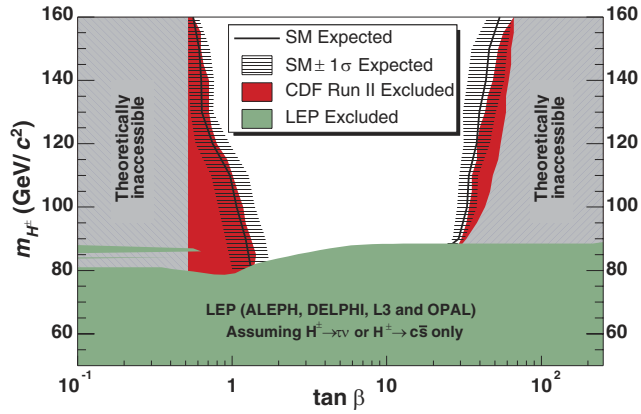


FIG. 2 (color online). The MSSM results obtained with 193 pb^{-1} at CDF. The SM-expected exclusion limits are indicated by black solid lines and the $\pm 1\sigma$ confidence band around it is obtained by generating pseudoexperiments. The darkest solid region represents the area excluded at 95% C.L. The solid lower region is the LEP combined results from direct searches [19]. Other relevant MSSM parameters are detailed in the caption of Fig. 1.

in the exclusion region shown in Fig. 2. We determine this exclusion region for several sets of benchmark parameters, including the maximal and minimal light Higgs mass scenarios described in Ref. [16]. The complete characterization of these scenarios and their results are described in Ref. [17]. In all the benchmarks used, the low $\tan\beta$ region is excluded in a similar region as shown in Fig. 2. The high $\tan\beta$ exclusion region, however, can be significantly reduced and even vanishes, due to parameters of particular benchmarks that suppress $\text{BR}(t \rightarrow H^+ b)$. The obtained exclusion limits strongly depend on the prior probability used. Using a flat prior in $\tan\beta$, which is characterized by sudden changes in the top and charged Higgs branching ratios, yields significantly different exclusion regions. It is important to note that, even if all the corrections were turned off and tree-level calculations were used, the results would be significantly stronger than those obtained in Ref. [8] under the same conditions.

In the high $\tan\beta$ region, the decay $H^+ \rightarrow \tau\nu$ is expected to dominate in a large fraction of the MSSM parameter space. In this region, the tauonic Higgs model is a good approximation, and we explicitly set $\text{BR}(H^+ \rightarrow \tau\nu) = 1$ and evaluate the posterior probability as a function of $\text{BR}(t \rightarrow H^+ b)$. The value of Γ_{H^\pm} has little effect on the results as width corrections to the efficiency are small; we set $\Gamma_{H^\pm} = 1.4 \text{ GeV}/c^2$. The width of the top is set to $\Gamma_t = 1.4 \text{ GeV}/c^2/[1 - \text{BR}(t \rightarrow H^+ b)]$, and the value of m_{h^0} is irrelevant in this model. We perform the scan in $\text{BR}(t \rightarrow H^+ b)$ from 0 to 1. A posterior probability density of $\text{BR}(t \rightarrow H^+ b)$ is obtained using a flat prior that is constant between 0 and 1 and null elsewhere. The 95% C.L. is obtained by integrating the posterior over the maximum density region. This procedure is repeated for different

charged Higgs masses. In the region $80 \text{ GeV}/c^2 \leq m_{H^\pm} \leq 160 \text{ GeV}/c^2$, we exclude $\text{BR}(t \rightarrow H^+ b) > 0.4$ at 95% C.L.

Finally, in order to reduce the model dependence, we place limits on $\text{BR}(t \rightarrow H^+ b)$ that hold for any combination of charged Higgs branching ratios. For a specific charged Higgs mass, we divide each of the five charged Higgs branching ratios into 21 bins. This results in 1771 possible branching ratio combinations subject to the relation $\sum_i \text{BR}(H^+ \rightarrow X_i) = 1$. For each combination, we obtain a limit on $\text{BR}(t \rightarrow H^+ b)$ assuming $\text{BR}(h^0 \rightarrow b\bar{b}) = 0.9$ and $m_{h^0} = 70 \text{ GeV}/c^2$. The least restrictive limit is quoted, and the analysis is repeated for different charged Higgs masses. The results are shown in Fig. 3. For $\text{BR}(t \rightarrow H^+ b) > 0.9$ (hatched region), the width of the top is larger than $14 \text{ GeV}/c^2$ and the analytical corrections to the efficiencies start losing accuracy.

In summary, we have performed a search for a charged Higgs boson in top quark decays using measurements of the top pair production cross section in four different final states, and we find no evidence of signal in the region $80 \text{ GeV}/c^2 \leq m_{H^\pm} \leq 160 \text{ GeV}/c^2$. In the context of the MSSM with full radiative corrections, we exclude the low $\tan\beta$ region for all benchmarks in Ref. [17]. The high $\tan\beta$ region cannot be excluded independent of the MSSM parameters. In the tauonic Higgs model, in which the

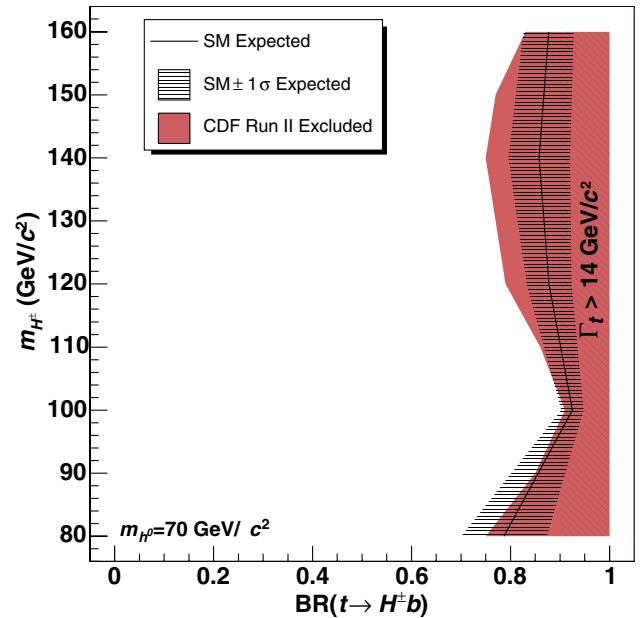


FIG. 3 (color online). Results for the charged Higgs branching ratio independent analysis with $m_t = 175 \text{ GeV}/c^2$. The dark solid region represents the CDF run II excluded region in the $[m_{H^\pm}, \text{BR}(t \rightarrow H^+ b)]$ plane. The expected exclusion limits are indicated by a black solid line and the $\pm 1\sigma$ confidence band around it is obtained by generating pseudoexperiments. The hatched region of $\text{BR}(t \rightarrow H^+ b) > 0.9$ indicates that the width of the top is larger than $14 \text{ GeV}/c^2$.

charged Higgs decays exclusively to $\bar{\tau}\nu$, the $\text{BR}(t \rightarrow H^+ b)$ is constrained to be less than 0.4 at 95% C.L. If no assumption is made on the charged Higgs decay, the $\text{BR}(t \rightarrow H^+ b)$ is constrained to be less than 0.91 at 95% C.L.

We thank the Fermilab staff and the technical staffs of the participating institutions for their vital contributions. This work was supported by the U.S. Department of Energy and National Science Foundation; the Italian Istituto Nazionale di Fisica Nucleare; the Ministry of Education, Culture, Sports, Science and Technology of Japan; the Natural Sciences and Engineering Research Council of Canada; the National Science Council of the Republic of China; the Swiss National Science Foundation; the A.P. Sloan Foundation; the Bundesministerium für Bildung und Forschung, Germany; the Korean Science and Engineering Foundation and the Korean Research Foundation; the Particle Physics and Astronomy Research Council and the Royal Society, UK; the Russian Foundation for Basic Research; the Comisión Interministerial de Ciencia y Tecnología, Spain; in part by the European Community's Human Potential Programme under Contract No. HPRN-CT-2002-00292; and the Academy of Finland.

-
- [1] P. W. Higgs, *Phys. Lett.* **12**, 132 (1964).
 - [2] M. Carena and H. E. Haber, *Prog. Part. Nucl. Phys.* **50**, 63 (2003).
 - [3] M. Cacciari *et al.*, *J. High Energy Phys.* 04 (2004) 068.
 - [4] We use a cylindrical coordinate system about the beam axis in which θ is the polar angle. We define transverse momentum $p_T = p \sin\theta$ and transverse energy E_T simi-

larly. Missing transverse energy ($\vec{\cancel{E}}_T$) is defined as $-\sum_i E_T^i \hat{n}_i$, where \hat{n}_i is the unit vector in the azimuthal plane that points from the $p\bar{p}$ interaction region to the i th calorimeter tower. $\vec{\cancel{E}}_T$ is further corrected for the energy and momentum of identified muons.

- [5] T. Affolder *et al.* (CDF Collaboration), *Phys. Rev. D* **62**, 012004 (2000).
- [6] F. Abe *et al.* (CDF Collaboration), *Phys. Rev. Lett.* **79**, 357 (1997).
- [7] V. M. Abazov *et al.* (D0 Collaboration), *Phys. Rev. Lett.* **88**, 151803 (2002).
- [8] B. Abbott *et al.* (D0 Collaboration), *Phys. Rev. Lett.* **82**, 4975 (1999).
- [9] M. Carena, D. Garcia, U. Nierste, and C. E. M. Wagner, *Nucl. Phys.* **B577**, 88 (2000).
- [10] A jet is determined to be tagged if it shows a displaced secondary vertex. These jets typically originate from the decay of long lived mesons such as those resulting after the hadronization process of the b quark.
- [11] D. Acosta *et al.* (CDF Collaboration), *Phys. Rev. Lett.* **93**, 142001 (2004).
- [12] A. Abulencia *et al.* (CDF Collaboration), hep-ex/0510063.
- [13] D. Acosta *et al.* (CDF Collaboration), *Phys. Rev. D* **71**, 052003 (2005).
- [14] T. Sjostrand *et al.*, *Comput. Phys. Commun.* **135**, 238 (2001).
- [15] J. S. Lee *et al.*, *Comput. Phys. Commun.* **156**, 283 (2004).
- [16] M. Carena, S. Heinemeyer, C. E. M. Wagner, and G. Weiglein, hep-ph/9912223.
- [17] R. Eusebi, Ph.D. thesis, University of Rochester, 2005.
- [18] For an introduction, see J. F. Gunion, H. Haber, G. Kane, and S. Dawson, *The Higgs Hunter's Guide*, Frontiers in Physics (Addison-Wesley, Redwood City, CA, 1989).
- [19] S. Eidelman *et al.* (Particle Data Group), *Phys. Lett. B* **592**, 1 (2004).